The Reagent [K(18-crown-6)][RuH(PPh$_3$)$_2$(η^5-7,8-C$_2$B$_9$H$_{11}$)] as a Precursor to New Ruthenacarborane Complexes†

Dianne D. Ellis,‡ Samantha M. Couchman,§ John C. Jeffery,§ John M. Malget,‡ and F. Gordon A. Stone*,‡

Department of Chemistry and Biochemistry, Baylor University, Waco, Texas 76798-7348, and School of Chemistry, The University, Bristol BS8 1TS, U.K.

Received January 7, 1999

In ethanol the charge-compensated molecule *exo-nido*-ruthenacarborane [5,6,10-{RuCl(PPh$_3$)$_2$}-5,6,10-μ-(H)$_3$-10-H-7,8-C$_2$B$_9$H$_8$] reacts with KOH to afford the anionic *closo*-complex [RuH(PPh$_3$)$_2$(η^5-7,8-C$_2$B$_9$H$_{11}$)]$^-$ isolated as its K$^+$ (**2a**) or [K(18-crown-6)]$^+$ (**2b**) salt. Treatment of **2a** with CO gives [Ru(CO)(PPh$_3$)$_2$(η^5-7,8-C$_2$B$_9$H$_{11}$)] (**3a**) in high yield; its structure was determined by X-ray crystallography. In contrast **2b** reacts with CO to yield the salt [K(18-crown-6)][RuH(CO)(PPh$_3$)(η^5-7,8-C$_2$B$_9$H$_{11}$)] (**2d**). Reaction of **2b** with [RuCl$_2$(PPh$_3$)$_3$] affords [Ru$_2$(μ-H)(H)(PPh$_3$)$_4$(η^5-7,8-C$_2$B$_9$H$_{11}$)] (**5**), which with CO produces [Ru$_2$(μ-H)(μ-σ: η^5-7,8-C$_2$B$_9$H$_{10}$)(CO)$_4$(PPh$_3$)$_2$] (**6**), the structure of which was established by X-ray diffraction. The molecule has a metal−metal bond bridged on one side by a hydrido ligand and on the other by a *nido*-7,8-C$_2$B$_9$H$_{10}$ fragment. The latter is η^5-coordinated to a ruthenium atom ligated by a PPh$_3$ and a CO ligand and is also σ-bonded to the second ruthenium which carries three CO molecules and a PPh$_3$ group. The σ bond utilizes a boron lying in an α site with respect to the carbons in the CC*B*BB ring coordinated to the Ru(CO)(PPh$_3$) moiety. Reactions between **2b** or **2d** and [CuCl(PPh$_3$)$_3$] and [AuCl(PPh$_3$)], respectively, afford the bimetal complexes [RuM(μ-H)(L)(PPh$_3$)$_2$(η^5-7,8-C$_2$B$_9$H$_{11}$)] [M = Cu, L = PPh$_3$ (**7a**), L = CO (**7b**); M = Au, L = PPh$_3$ (**8a**), L = CO (**8b**)]. X-ray diffraction studies are reported for **7a** and **8a**, revealing in the case of the former a structure in which an exopolyhedral B−H⇀Cu bond supplements the Ru(μ-H)Cu interaction.

Introduction

The ruthenacarborane tricarbonyl complex [Ru(CO)$_3$(η^5-7,8-C$_2$B$_9$H$_{11}$)] is a useful precursor for preparing a variety of organoruthenium compounds.[1] Products obtained from this reagent and its derivatives have unusual molecular structures because their η^5-7,8-C$_2$B$_9$H$_{11}$ ligands often adopt nonspectator roles. Reactivity of species having a 3,1,2-RuC$_2$B$_9$H$_{11}$ core structure would be expected to be influenced in part by the nature of the exopolyhedral ligands attached to the metal. We therefore considered complexes where CO molecules attached to the ruthenium center are replaced by PPh$_3$ in the expectation that species containing this more strongly donating group might be relatively nucleophilic both at the metal center and at one of the BH vertexes sited in the CCBBB ring ligating the ruthenium atom.[2] In this context a desirable candidate for study was the anionic hydrido complex [RuH(PPh$_3$)$_2$(η^5-7,8-C$_2$B$_9$H$_{11}$)]$^-$ since it should show nucleophilic behavior toward suitable electrophilic substrates. We have found the anion to be readily accessible as the potassium salt from the *exo-nido* charge-compensated ruthenacarborane complex [5,6,10-{RuCl(PPh$_3$)$_2$}-5,6,10-μ-(H)$_3$-10-H-7,8-C$_2$B$_9$H$_8$] (**1**), which in turn is conveniently prepared by treating [RuCl$_2$(PPh$_3$)$_3$] with [K][7,8-C$_2$B$_9$H$_{12}$].[3] During the course of our work the [NEt$_4$]$^+$ salt of the anion [RuH(PPh$_3$)$_2$(η^5-7,8-C$_2$B$_9$H$_{11}$)]$^-$ was independently prepared by others and characterized by an X-ray diffraction study.[4]

Results and Discussion

Treatment of compound **1** (Chart 1) with excess KOH in ethanol affords the thermally stable but air-sensitive salt [K][RuH(PPh$_3$)$_2$(η^5-7,8-C$_2$B$_9$H$_{11}$)] (**2a**) in essentially quantitative yield. The more stable salt [K(18-crown-6)][RuH(PPh$_3$)$_2$(η^5-7,8-C$_2$B$_9$H$_{11}$)] (**2b**) can be isolated microanalytically pure and

† The compounds described in this paper have a ruthenium atom incorporated into a *closo*-1,2-dicarba-3-ruthenadodecaborane framework. However, to avoid a complicated nomenclature for the complexes reported, and to relate them to the many known ruthenium species with η^5-coordinated cyclopentadienyl ligands, we treat the cages as *nido*-11-vertex ligands with numbering as for an icosahedron from which the twelfth vertex has been removed.

‡ Baylor University

§ Bristol University.

(1) (a) Anderson, S.; Mullica, D. F.; Sappenfield, E. L.; Stone, F. G. A. *Organometallics* **1995**, *14*, 3516. (b) Anderson, S.; Mullica, D. F.; Sappenfield, E. L.; Stone, F. G. A. *Organometallics* **1996**, *15*, 1676. (c) Anderson, S.; Jeffery, J. C.; Liao, Y.-H.; Mullica, D. F.; Sappenfield, E. L.; Stone, F. G. A. *Organometallics* **1997**, *16*, 958. (d) Jeffery, J. C.; Jelliss, P. A.; Psillakis, E.; Rudd, G. E. A.; Stone, F. G. A. *J. Organomet. Chem.* **1998**, *562*, 17. (e) Ellis, D.; Farmer, J. M.; Malget, J. M.; Mullica, D. F.; Stone, F. G. A. *Organometallics* **1998**, *17*, 5540. (f) Jeffery, J. C.; Jelliss, P. A.; Rudd, G. E. A.; Sakanishi, S.; Stone, F. G. A.; Whitehead, J. *J. Organomet. Chem.*, in press.

(2) (a) Jelliss, P. A.; Stone, F. G. A. *J. Organomet. Chem.* **1995**, *500*, 307. (b) Brew, S. A.; Stone, F. G. A. *Adv. Organomet. Chem.* **1993**, *35*, 135. (c) Stone, F. G. A. *Adv. Organomet. Chem.* **1990**, *31*, 53.

(3) Chizhevsky, I. T.; Lobanova, I. A.; Bregadze, V. I.; Petrovskii, P. V.; Antonovich, V. A.; Polyakov, A. V.; Yanovskii, A. I.; Struchkov, Y. T. *Mendeleev Commun.* **1991**, 47.

(4) Chizhevsky, I. T.; Lobanova, I. A.; Petrovskii, P. V.; Bregadze, V. I.; Dolgushin, F. M.; Yanovsky, A. I.; Struchkov, Y. T.; Chistyakov, A. L.; Stankevich, I. V.; Knobler, C. B.; Hawthorne, M. F. *Organometallics* **1999**, *18*, 726

10.1021/ic990057q CCC: $18.00
Published on Web 05/18/1999

Chart 1

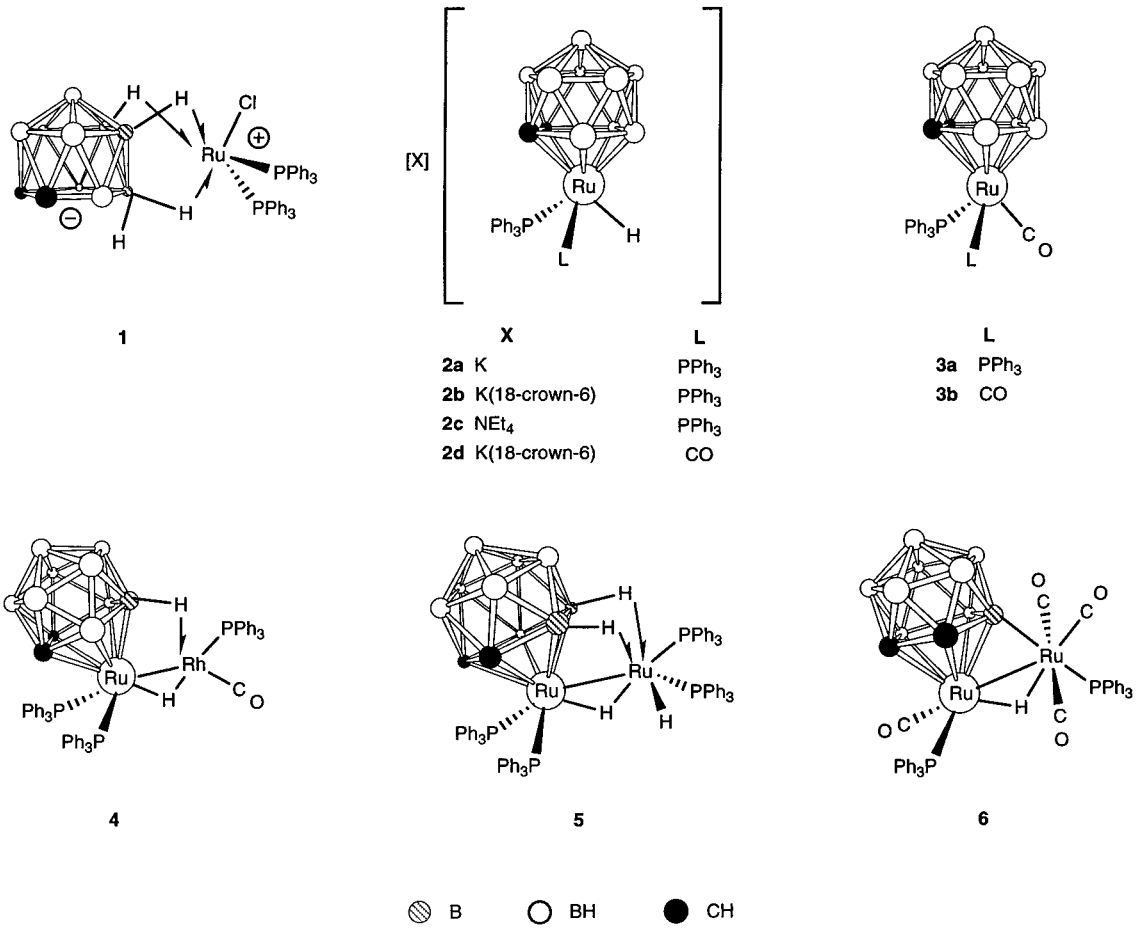

is conveniently prepared either in a direct synthesis from **1** and KOH using a variety of solvents (methanol, ethanol, *tert*-butyl alcohol, or thf) followed by addition of 18-crown-6, or by adding the crown ether to methanol solutions of **2a**. The NMR data for **2b** (Table 1) are very similar to those recently reported for $[NEt_4][RuH(PPh_3)_2(\eta^5\text{-}7,8\text{-}C_2B_9H_{11})]$ (**2c**), which was prepared in 84% yield from $[RuH(Cl)(PPh_3)_3]$ and $Tl_2[7,8\text{-}C_2B_9H_{11}]$ followed by addition of $[NEt_4]Cl$.[4]

The pathway by which **1** is converted into the salts **2a** and **2b** is obscure at present and indeed may vary with the solvent employed. It is unlikely in the first step that **1** converts via an oxidative addition process into the *closo*-complex $[RuH(Cl)(PPh_3)_2(\eta^5\text{-}7,8\text{-}C_2B_9H_{11})]$ since this conversion is reported to require elevated temperatures.[5] In contrast the salts **2a** and **2b** form in very high yields in room temperature reactions. It seems more probable that **1** is initially deprotonated by KOH to afford the anionic species $[RuCl(PPh_3)_2(\eta^5\text{-}7,8\text{-}C_2B_9H_{11})]^-$.[4] Replacement of the chloride ligand by OEt^- followed by the well-established β-elimination step for conversion of chloro−ruthenium complexes into hydrido species would yield the salt **2a** or **2b**. The formation of **2b** when thf or Bu^tOH is used requires these solvents to be the source of the hydride. There is precedent for this as Wilkinson and co-workers[6] have reported that $[Ru(H)_2(PPh_3)_4]$ is formed from $[RuH(Cl)(PPh_3)_3]$ upon treatment with KOH and Bu^tOH, and that $[RuCl_2(PPh_3)_3]$ and NaOH in refluxing thf afford $[Ru_2(H)_2(\mu\text{-}OH)_2(thf)_2(PPh_3)_4]$. Pathways were proposed for these reactions with the hydrido ligands derived from coordinated Bu^tOH or thf molecules.

The salt **2b** in CH_2Cl_2 reacts with CO at atmospheric pressure to give air-stable $[K(18\text{-crown-}6)][RuH(CO)(PPh_3)(\eta^5\text{-}7,8\text{-}C_2B_9H_{11})]$ (**2d**) in quantitative yield. NMR data for **2d** (Table 1) include a high-field diagnostic signal in the ^1H spectrum for the RuH group at δ −9.18 [J(PH) = 31 Hz]. The ruthenium atom is a chiral center; hence the cage CH groups give rise to two resonances in both the ^1H and $^{13}C\{^1H\}$ NMR spectra. The salts **2b** and **2d** are closely related to $[K(18\text{-crown-}6)][RuH(CO)_2(\eta^5\text{-}7,8\text{-}C_2B_9H_{11})]$, prepared originally by Behnken and Hawthorne,[7] and known to undergo a variety of reactions leading to other ruthenacarborane compounds.[1a,7]

Protonation of **2a** with HCl gives the dihydrido complex $[Ru(H)_2(PPh_3)_2(\eta^5\text{-}7,8\text{-}C_2B_9H_{11})]$. Interestingly we found that this dihydrido complex in MeOH with KOH and 18-crown-6 affords **2b**. Addition of excess HCl to **2a** slowly yields $[RuH(Cl)(PPh_3)_2(\eta^5\text{-}7,8\text{-}C_2B_9H_{11})]$. Both $[Ru(H)_2(PPh_3)_2(\eta^5\text{-}7,8\text{-}C_2B_9H_{11})]$ and $[RuH(Cl)(PPh_3)_2(\eta^5\text{-}7,8\text{-}C_2B_9H_{11})]$ were first obtained by Wong and Hawthorne,[8] the former via oxidative addition of $[RuH(Cl)(PPh_3)_3]$ with $[7,8\text{-}C_2B_9H_{12}]^-$, and the latter from $[Ru(H)_2(PPh_3)_2(\eta^5\text{-}7,8\text{-}C_2B_9H_{11})]$ and HCl gas.

Whereas **2b** reacts with CO to yield the salt **2d**, treating freshly prepared **2a** with CO in ethanol yields the complex $[Ru(CO)(PPh_3)_2(\eta^5\text{-}7,8\text{-}C_2B_9H_{11})]$ (**3a**) in ca. 90% yield. This provides a good synthesis for this species in further work since it may be accomplished in one step from **1** without the necessity

(5) Chizhevsky, I. T.; Yanovskii, A. I.; Struchkov, Y. T. *J. Organomet. Chem.* **1997**, *536*−*537*, 51.
(6) Chaudret, B. N.; Cole-Hamilton, D. J.; Nohr, R. S.; Wilkinson, G. *J. Chem. Soc., Dalton Trans.* **1977**, 1546.
(7) Behnken, P. E.; Hawthorne, M. F. *Inorg. Chem.* **1984**, *23*, 3420.
(8) Wong, E. H. S.; Hawthorne, M. F. *Inorg. Chem.* **1978**, *17*, 2863.

Table 1. Hydrogen-1, Carbon-13, Boron-11, and Phosphorus-31 NMR Data[a]

compd	$\delta(^1H)$[b]	$\delta(^{13}C)$[c]	$\delta(^{11}B)$[d]	$\delta(^{31}P)$[e]
2b	−9.83 [t, 1 RuH, *J*(PH) = 33], 1.66 (s, 2 H, cage CH), 3.60 (s, 24 H, OCH_2), 6.98−7.61 (m, 30 H, Ph)	140.7 [C^1(Ph)], 134.4−126.9 (Ph), 70.5 (OCH_2), 35.9 (cage CH)	−8.6 (1 B), −9.8 (1 B), −11.7 (1 B), −14.6 (3 B), −26.9 (3 B, br)	60.3 (s)
2d	−9.18 [d, 1 RuH, *J*(PH) = 31], 1.41 (s, 1 H, cage CH), 1.94 (s, 1 H, cage CH), 3.62 (s, 24 H, OCH_2), 7.35−7.16 (m, 30 H, Ph)	205.7 [d, RuCO, *J*(PC) = 18], 137.8 [C^1(Ph)], 133.8−128.4 (Ph), 70.5 (OCH_2), 38.4 (cage CH), 37.7 (cage CH)	−8.7 (1 B), −10.6 (1 B), −12.0 (2 B), −12.8 (2 B), −23.2 (1 B), −25.0 (2 B)	57.0 (s)
3a	2.21 (s, 2 H, cage CH), 7.17−7.33 (m, 30 H, Ph)	134.2 [C^1(Ph)], 133.9−128.5 (Ph), 47.1 (cage CH)[f]	1.6 (1 B), −2.4 (1 B), −8.2 (4 B), −20.3 (3 B)	41.1 (s)
5[g]	−15.63 [d of d, 1 Ru(μ-H)Ru, *J*(PH) = 31, 31], −9.72 [d of d, 1 RuH, *J*(PH) = 33, 33], −7.19 [br q × 2, 2 H, B−H⇀Ru, *J*(BH) = ca. 95], 1.63 (s, 2 H, cage CH), 7.04−7.48 (m, 30 H, Ph)		−6.0 (1 B, vbr), −7.9 (1 B, vbr), −9.7 (1 B, vbr), −18.1 (2 B), −21.2 (2 B), −27.1 (2 B)	71.5 [d, *J*(PP) = 30], 63.9 [d, *J*(PP) = 31], 61.6 [d, *J*(PP) = 31], 51.6 (vbr)
6	−13.88 [d of d, 1 H, Ru(μ-H)Ru, *J*(PH) = 16, 12[h]], 1.54 (s, 1 H, cage CH), 2.67 (s, 1 H, cage CH), 7.13−7.51 (m, 30 H, Ph)	134.4−126.9 (Ph)[i]	35.9 (1 B, RuB), 1.8 (2 B), −2.5 (1 B), −11.6 (1 B), −15.1 (2 B), −16.7 (1 B), −29.2 (1 B)	45.6 (s), 21.8 (s,br)
7a	−9.01 [d of t, 1 H, Cu(μ-H)Ru, *J*(P_{Cu}H) = 10, *J*(P_{Ru}H) = 25][j], 2.02 (s, 2 H, cage CH), 6.91−7.55 (m, 45 H, Ph)	137.8 [C^1(Ph)], 134.2−127.4 (Ph), 41.2 (cage CH)	−3.8 (1 B), −12.9 (4 B), −15.4 (1 B), −21.1 (1 B), −22.7 (2 B)	53.4 (s, 2 P, PRu), 3.8 (br s, 1 P, PCu)
7b[k]	−8.28 [br d, 1 H, Cu(μ-H)Ru, *J*(P_{Ru}H) = 21][j], 1.97 (s, 1 H, cage CH), 2.09 (s, 1 H, cage CH), 7.28−7.54 (m, 30 H, Ph)	199.1 [d, CO, *J*(PC) = 18] 134.8−128.7 (Ph), 46.6, 37.1 (cage CH)	−3.8 (1 B), −8.4 (2 B), −12.9 (1 B), −13.8 (2 B), −18.3 (1 B), −19.1 (1 B), −25.1 (2 B)	53.5 (s, 1 P, PRu), 6.2 (br s, 1 P, PCu)
8a	−5.88 [d of t, 1 H, Au(μ-H)Ru, *J*(P_{Au}H) = 57, *J*(P_{Ru}H) = 22], 2.10 (s, 2 H, cage CH), 6.99−7.62 (m, 45 H, Ph)	137.4 [C^1(Ph)] 134.4−127.4 (Ph), 42.4 (cage CH)	−0.9 (1 B), −6.3 (1 B), −9.2 (1 B), −11.5 (3 B), −23.7 (3 B)	50.7 (s, 2 P, RuP), 42.0 (br s, 1 P, AuP)
8b[k]	−5.01 [d of d, 1 H, Au(μ-H)Ru, *J*(P_{Au}H) = 70, *J*(P_{Ru}H) = 20], 2.15 (s, 1 H, cage CH), 2.84 (s, 1 H, cage CH), 7.34−7.64 (m, 30 H, Ph)	203.6 [d, CO, *J*(PC) = 20] 135.1−128.7 (Ph), 45.8, 44.0 (cage CH)	0.2 (1 B), −4.3 (1 B), −8.3 (1 B), −9.4 (1 B), −10.5 (1 B), −12.2 (1 B), −21.7 (3 B)	54.0 (s, 2 P, PRu), 47.0 (br s, 1 P, PAu)

[a] Chemical shifts (δ) in parts per million, coupling constants (*J*) in hertz, measurements in CD_2Cl_2 at room temperature. [b] Signals for BH protons not exopolyhedrally bridge bonded occur as broad unresolved signals in the range (δ) −1 to 2.5. [c] Hydrogen-1 decoupled, chemical shifts are positive to high frequency of $SiMe_4$. [d] Hydrogen-1 decoupled, chemical shifts are positive to high frequency of BF_3·Et_2O (external). [e] Hydrogen-1 decoupled; chemical shifts are positive to high frequency of 85% H_3PO_4 (external). [f] Complex insoluble, spectrum too weak to observe CO and cage CH peaks. [g] ^{13}C spectrum not measured due to sample decomposition. [h] Couplings obtained from selective $^1H\{^{31}P\}$ spectrum. [i] Spectrum weak, resonance for CO with ^{31}P coupling not observed. [j] Resonance for B−H⇀Cu too broad to be observed. [k] $^{13}C\{^1H\}$ and ^{1}H spectra measured at 280 K.

Table 2. Selected Internuclear Distances (Å) and Angles (deg) for [Ru(CO)(PPh$_3$)$_2$(η^5-7,8-C$_2$B$_9$H$_{11}$)] (**3a**)

Ru−C	1.854(3)	Ru−C(1)	2.245(3)	Ru−B(4)	2.298(3)	Ru−C(2)	2.277(3)
Ru−B(3)	2.283(3)	Ru−B(5)	2.284(3)	Ru−P(2)	2.3873(7)	Ru−P(1)	2.4021(7)
C−O	1.148(3)	P(1)−C(21)	1.843(3)	P(1)−C(31)	1.844(3)	P(1)−C(41)	1.846(3)
P(2)−C(71)	1.835(3)	P(2)−C(61)	1.840(3)	P(2)−C(51)	1.835(3)		

C−Ru−C(1)	116.43(11)	C−Ru−B(3)	133.12(11)	C−Ru−C(2)	156.46(11)
C−Ru−B(4)	90.19(11)	C−Ru−P(2)	88.10(8)	C−Ru−B(5)	81.44(12)
C(1)−Ru−B(3)	74.43(10)	C(1)−Ru−C(2)	42.62(10)	C(2)−Ru−B(3)	43.25(10)
C(2)−Ru−B(5)	75.12(11)	C(1)−Ru−B(5)	44.78(11)	B(3)−Ru−B(5)	77.84(11)
C(2)−Ru−B(4)	75.40(10)	C(1)−Ru−B(4)	76.49(11)	B(3)−Ru−B(4)	45.91(11)
B(5)−Ru−B(4)	46.84(10)	C(1)−Ru−P(2)	154.85(8)	C(2)−Ru−P(2)	112.23(7)
B(3)−Ru−P(2)	84.80(8)	B(4)−Ru−P(2)	99.23(8)	B(5)−Ru−P(2)	143.97(8)
C−Ru−P(1)	93.32(9)	C(1)−Ru−P(1)	84.31(8)	C(2)−Ru−P(1)	94.35(7)
B(3)−Ru−P(1)	133.54(8)	B(4)−Ru−P(1)	159.96(8)	B(5)−Ru−P(1)	114.29(8)
O−C−Ru	172.8(3)	P(2)−Ru−P(1)	100.60(3)		

of isolating **2a**. Compound **3a** was previously obtained, in 45% and 20% yields, respectively, from the reaction between [Ru(H)$_2$(PPh$_3$)$_2$(η^5-7,8-C$_2$B$_9$H$_{11}$)] and CO at 100 °C[8] and by treating [RuCl$_2$(CO)$_2$(PPh$_3$)$_2$] with [Na]$_2$[7,8-C$_2$B$_9$H$_{11}$].[9]

Formation of the neutral species **3a** from the salt **2a** was unexpected. For this reason we confirmed the nature of **3a** by an X-ray diffraction study. Selected bond distances and angles are given in Table 2, and the molecule is shown in Figure 1. As expected the ruthenium is η^5-coordinated on one side by the *nido*-7,8-C$_2$B$_9$H$_{11}$ cage and on the other by two PPh$_3$ groups and a CO molecule. The pathway by which **3a** forms from **2a** and CO is presently obscure.

The *exo-nido*-complex **1** reacts with [Rh$_2$(μ-Cl)$_2$(CO)$_4$] in the presence of KOH and MeOH to afford the bimetal complex [RuRh(μ-H)(CO)(PPh$_3$)$_3$(η^5-7,8-C$_2$B$_9$H$_{11}$)] (**4**) together with small amounts of **3a** (5%) and **3b** (3%).[4] The anionic complex [RuH(PPh$_3$)$_2$(η^5-7,8-C$_2$B$_9$H$_{11}$)]$^-$ was implicated as an intermediate in this synthesis. In support of this proposal we find that **4** can be obtained in high yield by treating the well-defined salt **2b** with [RhCl(CO)(PPh$_3$)$_2$] in ethanol. Compound **2d** is a minor product of the reaction, implying transfer of CO to ruthenium with concomitant displacement of PPh$_3$. In the previous synthesis of **4** the rhodium compound employed was [Rh$_2$(μ-Cl)$_2$(CO)$_4$], and as mentioned above the complexes [Ru(CO)(L)(PPh$_3$)(η^5-7,8-C$_2$B$_9$H$_{11}$)] [L = PPh$_3$ (**3a**), CO (**3b**)] were formed as side products as a result of CO ligand transfer to ruthenium. Clearly PPh$_3$ transfer to rhodium was also involved in the earlier synthesis of **4** since [Rh$_2$(μ-Cl)$_2$(CO)$_4$] was the precursor.

When gently warmed in ethanol, **2b** reacts with [RuCl$_2$(PPh$_3$)$_3$] to give a diruthenium complex best formulated as [Ru$_2$-

(9) Siedle, A. R. *J. Organomet. Chem.* **1975**, *90*, 249.

Table 3. Selected Internuclear Distances (Å) and Angles (deg) for $[Ru_2(\mu\text{-H})(\mu\text{-}\sigma\text{:}\eta^5\text{-7,8-}C_2B_9H_{10})(CO)_4(PPh_3)_2]\cdot CH_2Cl_2$ (**6**)

Ru(1)−C(11)	1.850(2)	Ru(1)−B(3)	2.159(3)	Ru(1)−C(1)	2.253(2)	Ru(1)−C(2)	2.230(2)
Ru(1)−B(4)	2.282(3)	Ru(1)−B(5)	2.281(3)	Ru(1)−P(3)	2.3653(7)	Ru(1)−Ru(2)	2.9536(6)
Ru(1)−H(3)	1.76(2)	Ru(2)−C(21)	1.939(2)	Ru(2)−C(23)	1.894(2)	Ru(2)−C(22)	1.958(2)
Ru(2)−B(3)	2.164(3)	Ru(2)−P(4)	2.4428(7)	Ru(2)−H(3)	1.87(2)	P(3)−C(311)	1.839(2)
P(3)−C(331)	1.824(2)	P(3)−C(321)	1.836(2)	P(4)−C(431)	1.832(2)	P(4)−C(411)	1.833(2)
P(4)−C(421)	1.823(2)	C(11)−O(11)	1.153(3)	C(21)−O(21)	1.136(3)	C(22)−O(22)	1.131(3)
C(23)−O(23)	1.135(3)						

C(11)−Ru(1)−B(3)	126.41(10)	C(11)−Ru(1)−C(1)	125.91(9)	C(11)−Ru(1)−C(2)	163.20(10)
B(3)−Ru(1)−C(1)	77.54(9)	B(3)−Ru(1)−C(2)	47.53(9)	C(2)−Ru(1)−C(1)	42.01(8)
C(11)−Ru(1)−B(4)	87.28(10)	C(1)−Ru(1)−B(4)	76.92(9)	B(3)−Ru(1)−B(4)	48.10(9)
C(2)−Ru(1)−B(4)	78.59(9)	C(11)−Ru(1)−B(5)	88.12(10)	B(3)−Ru(1)−B(5)	80.58(10)
C(2)−Ru(1)−B(5)	75.61(9)	B(4)−Ru(1)−B(5)	46.78(9)	C(1)−Ru(1)−B(5)	44.35(9)
C(1)−Ru(1)−P(3)	92.55(6)	C(2)−Ru(1)−P(3)	100.17(6)	B(4)−Ru(1)−P(3)	165.70(7)
B(5)−Ru(1)−P(3)	118.97(7)	B(3)−Ru(1)−P(3)	139.57(7)	C(11)−Ru(1)−P(3)	91.26(7)
B(3)−Ru(1)−Ru(2)	46.98(7)	C(11)−Ru(1)−Ru(2)	107.15(7)	C(2)−Ru(1)−Ru(2)	79.52(6)
C(1)−Ru(1)−Ru(2)	120.02(6)	B(5)−Ru(1)−Ru(2)	124.42(7)	B(4)−Ru(1)−Ru(2)	80.09(7)
P(3)−Ru(1)−Ru(2)	113.86(2)	C(23)−Ru(2)−C(21)	90.33(10)	C(23)−Ru(2)−C(22)	88.16(10)
C(21)−Ru(2)−C(22)	174.11(9)	C(21)−Ru(2)−B(3)	88.32(9)	C(23)−Ru(2)−B(3)	91.50(10)
C(22)−Ru(2)−B(3)	86.03(9)	C(23)−Ru(2)−P(4)	101.55(7)	C(21)−Ru(2)−P(4)	95.90(7)
C(22)−Ru(2)−P(4)	89.98(7)	B(3)−Ru(2)−P(4)	166.23(7)	C(21)−Ru(2)−Ru(1)	87.23(7)
C(22)−Ru(2)−Ru(1)	90.12(7)	C(23)−Ru(2)−Ru(1)	138.30(7)	B(3)−Ru(2)−Ru(1)	46.84(7)
P(4)−Ru(2)−Ru(1)	120.11(2)	Ru(1)−B(3)−Ru(2)	86.18(9)	O(11)−C(11)−Ru(1)	173.7(2)
O(22)−C(22)−Ru(2)	176.3(2)	O(21)−C(21)−Ru(2)	177.2(2)	O(23)−C(23)−Ru(2)	176.4(2)

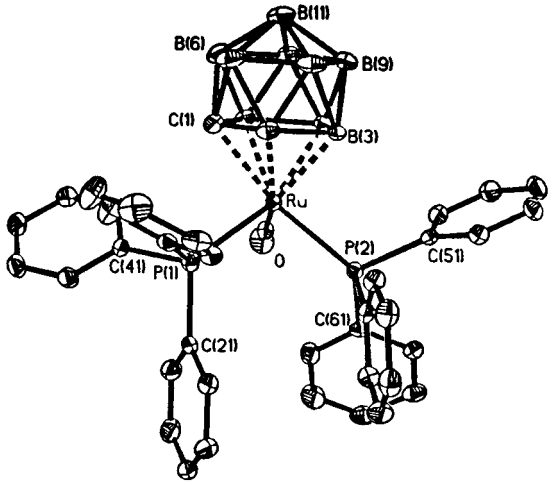

Figure 1. Molecular structure of $[Ru(CO)(PPh_3)_2(\eta^5\text{-7,8-}C_2B_9H_{11})]$ (**3a**) showing the crystallographic atom-labeling scheme. Thermal ellipsoids are shown at the 40% probability level. Hydrogen atoms are omitted for clarity.

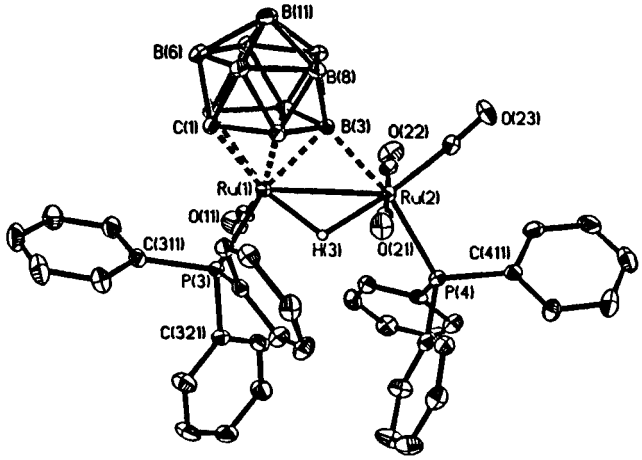

Figure 2. Molecular structure of $[Ru_2(\mu\text{-H})(\mu\text{-}\sigma,\eta^5\text{-7,8-}C_2B_9H_{10})(CO)_4(PPh_3)_2]$ (**6**) showing the crystallographic atom-labeling scheme. Thermal ellipsoids are shown at the 40% probability level. Except for H(3), the hydrogen atoms are omitted for clarity.

$(\mu\text{-H})(H)(PPh_3)_4(\eta^5\text{-7,8-}C_2B_9H_{11})]$ (**5**) on the basis of its NMR spectra (Table 1). Unfortunately, **5** was air-sensitive and crystals could not be obtained for an X-ray diffraction study. Moreover, in solution it converts into a new and presently unidentified dark pink complex. Accordingly repeated attempts to obtain samples of sufficient purity for elemental analysis were unsuccessful. However, the ^1H NMR spectrum reveals diagnostic resonances for a Ru(μ-H)Ru proton and a terminal hydrido ligand at δ −15.63 and −9.72,[10] respectively. There is also a very broad quartet corresponding in intensity to two protons at δ −7.19 [J(BH) = 95 Hz] characteristic of agostic B−H⇀Ru groups.[2b] The $^{31}P\{^1H\}$ was also informative with resonances for four nonequivalent phosphorus ligands (Table 1). Three signals were doublets [J(PP) ≈ 30 Hz], and the third peak was very broad, probably due to $^{11}B-^{31}P$ coupling, as is likely since one PPh_3 group lies transoid to a cage boron nucleus.

In an attempt to obtain a more stable derivative, **5** was treated in CH_2Cl_2 with CO. This reaction gave the diruthenium complex $[Ru_2(\mu\text{-H})(\mu\text{-}\sigma\text{:}\eta^5\text{-7,8-}C_2B_9H_{10})(CO)_4(PPh_3)_2]$ (**6**) in essentially quantitative yield. Fortunately, good-quality crystals were available for an X-ray diffraction study because the molecular structure could not be fully deduced from the NMR data. The molecule **6** is shown in Figure 2, and selected bond distances and angles are listed in Table 3.

The Ru(1)−Ru(2) bond [2.9356(6) Å] is bridged by the hydrido ligand H(3), which was located in the difference Fourier syntheses and its position refined. On the other side of the metal−metal bond the *nido*-7,8-C_2B_9 framework is η^5-coordinated to Ru(1) and forms a σ bond [2.164(3) Å] between B(3) and Ru(2). This mode of attachment of *nido*-7,8-R_2-7,8-$C_2B_9H_8$ (R = H or Me) fragments to dimetal systems is now known to be common and has been confirmed by several X-ray diffraction studies made in recent years.[2] Of interest, however, in these structures is whether the σ bond from the boron to the metal atom which is exopolyhedrally attached to the *closo*-3,1,2-MC_2B_9 cage system is from an α- or a β-boron with respect to the carbons in the CCBBB ring ligating M. For molecule **6** it is B(3) lying in an α site which forms the B−Ru bond. This is in contrast with the situation in the anion of $[N(PPh_3)_2][WRu(\mu\text{-}CC_6H_4Me\text{-}4)(\mu\text{-}\sigma\text{:}\eta^5\text{-7,8-}Me_2\text{-7,8-}C_2B_9H_8)(CO)_3(\eta^5\text{-}C_5H_5)]$ [B−Ru

(10) Kaesz, H. D.; Saillant, R. B. *Chem. Rev.* **1972**, *72*, 231.

Chart 2

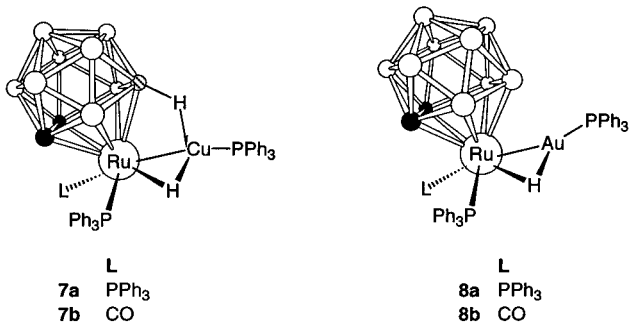

	L
7a	PPh_3
7b	CO

	L
8a	PPh_3
8b	CO

= 2.155(6) Å].[11] The latter is formed by deprotonation of a neutral species with an exopolyhedral B$_\beta$−H⇀Ru linkage. Formation of exopolyhedral B−H⇀M′ linkages in dimetal M−M′ systems is frequently followed by an intramolecular oxidative addition to yield B−M′ and M(μ-H)M′ bonds as apparently occurs in the formation of compound **6** from **5**. A B$_\alpha$−H⇀Ru linkage is evidently involved in this step in order to afford the B(3)−Ru(2) bond (Figure 2), but the process is complicated by loss of a molecule of hydrogen. Atom Ru(1) in **6** is coordinated by a PPh_3 group and a CO molecule, while Ru(2) is ligated by a PPh_3 group transoid to B(3) [B(3)−Ru(2)-P(4) = 166.23(7)°] and by three meridional CO molecules. Overall the dimetal complex has 34 valence electrons and is thus electronically saturated.

The structure of **6** having been determined, the NMR data (Table 1) are readily interpretable. In the ^{1}H NMR spectrum the signal for the Ru(μ-H)Ru group is seen as a doublet of doublets at δ −13.88. Because of the asymmetry of the molecule, two resonances are seen for the cage CH protons, the chemical shifts (δ 1.54 and 2.67) being in the expected range.[2b] Unfortunately the insolubility of complex **6** prevented the acquisition of meaningful ^{13}C{^{1}H} data. However, the ^{11}B{^{1}H} spectrum revealed a diagnostic resonance for B(3) at δ 35.9 which remained a singlet in a fully coupled ^{11}B spectrum.[2b] As expected the ^{31}P{^{1}H} NMR spectrum of **5** revealed two peaks for the nonequivalent PPh_3 ligands. These occur at δ 45.6 and 21.8 and, on the basis of the shifts, may be assigned to P(3) and P(4), respectively.[1b] Moreover, the latter is as expected broad due to incipient ^{11}B−^{31}P coupling since the P(4) nucleus is transoid to B(3).

We recently reported[1a] that the reaction between [K(18-crown-6)][RuH(CO)$_2$(η^5-7,8-C$_2$B$_9$H$_{11}$)] and [AuCl(PPh_3)] afforded [Au(PPh_3)$_2$][RuCl(CO)$_2$(η^5-7,8-C$_2$B$_9$H$_{11}$)] instead of a species with a Ru−Au bond as was expected. This led us to consider the products that might be obtained by treating the salts **2b** and **2d** with the complexes [AuCl(PPh_3)] and [CuCl(PPh_3)$_3$], respectively. These reactions yielded the bimetallic complexes [RuCu(μ-H)(L)(PPh_3)$_2$(η^5-7,8-C$_2$B$_9$H$_{11}$)] [L = PPh_3 (**7a**); CO (**7b**)] and [RuAu(μ-H)(L)(PPh_3)$_2$(η^5-7,8-C$_2$B$_9$H$_{11}$)] [L = PPh_3 (**8a**); CO (**8b**)] in excellent yields.

Of immediate interest was the manner in which the Cu(PPh_3) and Au(PPh_3) units in the molecules **7** and **8** (Chart 2) were attached to the *closo*-3,1,2-RuC$_2$B$_9$ cages. Many complexes are known having copper- or gold-containing fragments exopolyhedrally attached to the metal vertexes of *closo*-3,1,2-MC$_2$B$_9$ or *closo*-2,1-MCB$_{10}$ metallacarborane frameworks.[2a] In the copper species the M−Cu bonds are usually supplemented by one or two agostic B−H⇀Cu interactions involving BH groups

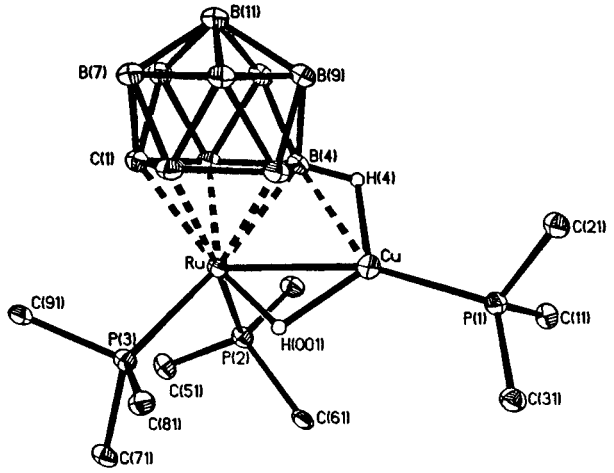

Figure 3. Molecular structure of [RuCu(μ-H)(PPh_3)$_3$(η^5-7,8-C$_2$B$_9$H$_{11}$)] (**7a**) showing the crystallographic atom-labeling scheme. Thermal ellipsoids are shown at the 40% probability level. Except for H(4) and H(001), the hydrogen atoms and phenyl groups are omitted for clarity.

in the pentagonal CCBBB and CBBBB rings pentahapto coordinated to the metal centers.[12,13] In contrast *closo*-icosahedral metallacarboranes having both exopolyhedral M−Au and B−H⇀Au bonds are much less common.[14] Unfortunately diagnostic resonances for B−H⇀Cu(Au) linkages are often impossible to detect by ^{1}H or ^{11}B NMR spectroscopy due to their broadness, a feature that has been attributed to dynamic behavior in solution involving a fast exchange between B−H⇀Cu(Au) sites on the NMR time scale or the loss of signals in the background noise due to the quadrupolar effect of the boron, enhanced by the ^{63}Cu and ^{197}Au nuclei with spin $I = {}^3/_2$.[13b] Thus, although the ^{1}H and ^{11}B NMR data (Table 1) for compounds **7** and **8** provided no evidence for the presence of agostic B−H⇀Cu(Au) bonding, this could not be taken as indicating the absence of such bonding. Hence recourse had to be made to X-ray crystallographic studies to establish the structures at least in the solid state.

The molecules studied crystallographically were **7a**, **7b**, and **8a**. The structures of **7a** and **8a** are shown in Figures 3 and 4, and selected bond distances and angles are listed in Tables 4 and 5, respectively. Because the structure of **7b** is so similar to that of **7a**, apart from replacement of a PPh_3 group on the ruthenium by CO, the results are given in the Supporting Information.

It is immediately apparent that molecule **7a** has a two-point attachment of the Cu(PPh_3) moiety to the *closo*-3,1,2-RuC$_2$B$_9$H$_{11}$ cage framework. The attachments comprise a Ru−H(001)−Cu bridge system [Ru−Cu 2.5758(6) Å, Ru−H(001) 1.60(4) Å, Cu−H(001) 1.89(4) Å] and a B(4)−H(4)⇀Cu three-center two-electron bond [B(4)−Cu 2.215(4) Å, Cu−H(4) 1.89(4) Å]. The latter involves the boron B(4) lying in the β site with respect to the carbons in the CCB*B*B ring ligating the ruthenium atom. Interestingly, in **7b** a β-boron atom is also involved in the B−H⇀Cu linkage, a feature that also could not be established

(11) Green, M.; Howard, J. A. K.; Jelfs, A. N. de M.; Johnson, O.; Stone, F. G. A. *J. Chem. Soc., Dalton Trans.* **1987**, 73.

(12) Do, Y.; Knobler, C. B.; Hawthorne, M. F. *J. Am. Chem. Soc.* **1987**, *109*, 1853. Kang, H. C.; Do, Y.; Knobler, C. B.; Hawthorne, M. F. *Inorg. Chem.* **1988**, *27*, 1716.

(13) (a) Cabioch, J.-L.; Dossett, S. J.; Hart, I. J.; Pilotti, M. U.; Stone, F. G. A. *J. Chem. Soc., Dalton Trans.* **1991**, 519. (b) Batten, S. A.; Jeffrey, J. C.; Jones, P. L.; Mullica, D. F.; Rudd, M. D.; Sappenfield, E. L.; Stone, F. G. A.; Wolf, A. *Inorg. Chem.* **1997**, *36*, 2570.

(14) Carr, N.; Gimeno, M. C.; Goldberg, J. E.; Pilotti, M. U.; Stone, F. G. A.; Topaloğlu, I. *J. Chem. Soc., Dalton Trans.* **1990**, 2253. Jeffery, J. C.; Jelliss, P. A.; Stone, F. G. A. *Organometallics* **1994**, *13*, 2651.

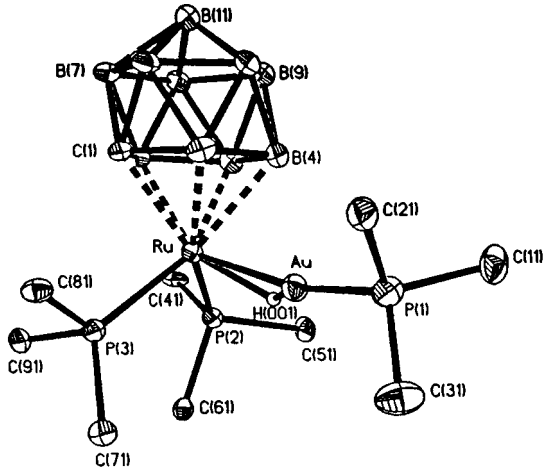

Figure 4. Molecular structure of $[RuAu(\mu\text{-}H)(PPh_3)_3(\eta^5\text{-}7,8\text{-}C_2B_9H_{11})]$ (**8a**) showing the crystallographic atom-labeling scheme. Thermal ellipsoids are shown at the 40% probability level. Except for H(001), the hydrogen atoms and the phenyl groups on phosphorus are omitted for clarity.

by NMR spectroscopy. The bonding between the two fragments $RuH(PPh_3)_2(\eta^5\text{-}7,8\text{-}C_2B_9H_{11})$ and $Cu(PPh_3)$ may be viewed in two ways: (i) A Ru−Cu bond is bridged by a hydrido ligand, and this linkage is supplemented by the B−H⇀Cu three-center two-electron bond. The cage system contributes three electrons to the copper, which overall has a 16e valence shell. (ii) The molecule is zwitterionic with the 18e anion $[RuH(PPh_3)_2(\eta^5\text{-}7,8\text{-}C_2B_9H_{11})]^-$ formally donating four electrons via B−H⇀Cu and Ru−H⇀Cu bonds to a cationic 12e $[Cu(PPh_3)]^+$ fragment. This would imply the absence of a direct metal−metal bond.[4] However, the observed Ru−Cu distance in **7a** [2.5758(6) Å] is similar to those found in ruthenium carbonyl clusters containing $Cu(PPh_3)$ groups;[15] hence there seems little reason to prefer bonding formulation ii in preference to i at the present time.

In the gold complex **8a** (Figure 4) there is no exopolyhedral B−H⇀Au bond supplementing the Ru(μ-H)Au linkage [Ru−Au 2.7205(8) Å, Ru−H(001) 1.79(6) Å, Au−H(001) 1.37(5) Å]. These distances compare well with those found in the cation $[RuAu(\mu\text{-}H)_2(CO)(PPh_3)_4]^+$ [Ru−Au 2.786(1) Å, Ru−H 1.78(4) Å, Au−H 1.61(4) Å].[16] The absence of an agostic B−H⇀Au interaction in **8a** and the presence of the B−H⇀Cu linkage in **7a** can be related to the relative differences in the energies of the unoccupied frontier orbitals in the fragments $M(PPh_3)$ (M = Cu or Au). For copper the valence hybrid sp_z orbital and the degenerate pair of p_x and p_y orbitals are sufficiently close to make all three available for bonding whereas with gold the p_x and p_y orbitals are generally less accessible for bonding,[17,18] hence the preference of copper to increase its coordination number relative to gold in these complexes.

Conclusions

The results described herein show that the salt $[K(18\text{-crown-}6)][RuH(PPh_3)_2(\eta^5\text{-}7,8\text{-}C_2B_9H_{11})]$ (**2b**) can be prepared in very high yield and used to synthesize compounds with Ru−Ru, Ru−Cu, and Ru−Au bonds. A new and high-yield route to $[Ru(CO)(PPh_3)_2(\eta^5\text{-}7,8\text{-}C_2B_9H_{11})]$ (**3a**) is also now available.

Experimental Section

General Considerations. All reactions were performed under an atmosphere of dry nitrogen using standard Schlenk line techniques. Solvents were distilled from appropriate drying agents under an atmosphere of dry nitrogen or argon and thoroughly purged with nitrogen prior to use. Petroleum ether refers to that fraction of boiling point 40−60 °C. NMR spectra were recorded at the following frequencies (MHz): ^1H at 360.13, $^{13}C\{^1H\}$ at 90.56, $^{31}P\{^1H\}$ at 145.78, $^{11}B\{^1H\}$ at 115.5. $^{31}P\{^1H\}$ NMR shifts are quoted in the text to high field of 85% H_3PO_4 (external). The reagents $[5,6,10\text{-}\{RuCl(PPh_3)_2\}\text{-}5,6,10\text{-}\mu\text{-}(H)_3\text{-}10\text{-}H\text{-}7,8\text{-}C_2B_9H_8]$,[3] $[RuCl_2(PPh_3)_3]$,[19a] and $[RhCl(CO)(PPh_3)_2]$[19b] were prepared according to literature methods.

Synthesis of $[K][RuH(PPh_3)_2(\eta^5\text{-}7,8\text{-}C_2B_9H_{11})]$. Excess KOH (ca. 150 mg) was added to **1** (100 mg, 0.13 mmol), and the Schlenk tube containing the two reagents was evacuated for 2 h. Ethanol (nondistilled, 10 mL) was then added and the suspension stirred for 12 h. The resultant bright yellow precipitate was filtered under nitrogen and washed successively with H_2O (2 × 10 mL), chilled EtOH (1 × 10 mL), and Et_2O (1 × 10 mL) and the residue dried in vacuo to afford $[K][RuH(PPh_3)_2(\eta^5\text{-}7,8\text{-}C_2B_9H_{11})]$ (**2a**) (103 mg). The NMR spectra (Table 1) of samples thus obtained revealed the presence of EtOH molecules which probably ligate the cation. Solutions of **2a** are very air-sensitive.

Synthesis of $[K(18\text{-crown-}6)][RuH(PPh_3)_2(\eta^5\text{-}7,8\text{-}C_2B_9H_{11})]$. Compound **1** (100 mg, 0.13 mmol) and excess KOH (ca. 150 mg) were placed in a Schlenk tube, which was evacuated for 2 h to remove all traces of oxygen. Absolute methanol (10 mL) and 18-crown-6 (37 mg, 0.14 mmol) were added, and the suspension was slowly stirred for 15 h. After cooling to ca. 0 °C, the yellow microcrystals were isolated by filtration, washed with H_2O (2 × 10 mL) and MeOH (1 × 10 mL), and dried in vacuo to afford $[K(18\text{-crown-}6)][RuH(PPh_3)_2(\eta^5\text{-}7,8\text{-}C_2B_9H_{11})]$ (**2b**) (130 mg, 97%). This product was sufficiently pure for subsequent investigations. Slow diffusion of thf solutions of **2b** into a methanol layer at 0 °C gives spectroscopically pure bright yellow plates after washing with petroleum ether (1 × 5 mL) and drying in vacuo. However, solutions of the complex are air-sensitive. It crystallizes with a molecule of thf. Calcd for $C_{50}H_{66}B_9KO_6P_2Ru\cdot C_4H_8O$: C, 57.7; H, 7.0. Found: C, 57.2; H, 6.6.

Synthesis of $[K(18\text{-crown-}6)][RuH(CO)(PPh_3)(\eta^5\text{-}7,8\text{-}C_2B_9H_{11})]$. Compound **2b** (50 mg, 0.047 mmol) was dissolved in CH_2Cl_2 (5 mL) and slowly stirred under an atmosphere of CO for 15 h. During this time the solution became pale yellow. Solvent was removed in vacuo and the semisolid washed with Et_2O (2 × 10 mL) to afford a cream solid, which was dried in vacuo to give $[K(18\text{-crown-}6)][RuH(CO)(PPh_3)(\eta^5\text{-}7,8\text{-}C_2B_9H_{11})]$ (**2d**) (38 mg, 99%). The compound thus obtained is spectroscopically pure. Analytically pure samples were obtained by recrystallization from $CH_2Cl_2-Et_2O$ solutions. Calcd for $C_{33}H_{51}B_9KO_7PRu$: C, 47.9; H, 6.2. Found: C, 47.8; H, 6.2.

Synthesis of $[Ru(CO)(PPh_3)_2(\eta^5\text{-}7,8\text{-}C_2B_9H_{11})]$. A Schlenk tube was charged with compound **1** (500 mg, 0.63 mmol) and excess KOH (ca. 300 mg), and the reagents were pumped under vacuum for 2 h. Absolute ethanol (50 mL) was then added and the suspension stirred for 12 h, generating a bright yellow solution of **2a**. The atmosphere was then changed to CO and the solution brought to a brisk reflux for 1−2 days, resulting in the gradual precipitation of a pale yellow solid. Note: Admission of air at this stage results in a greatly reduced yield of final product, decomposition being revealed by the appearance of a brown coloration. The resultant pale yellow solid was dissolved in CH_2Cl_2 (ca. 15 mL) and passed through silica (20 × 100 mm) with Et_2O as eluant, only the major bright yellow fraction being collected. Solvent was removed in vacuo, and the semisolid residue was dissolved in CH_2Cl_2, whereupon diffusion into a Et_2O layer at 25 °C gave yellow blocks, which were washed with ethanol (2 × 10 mL) and petroleum ether (1 × 10 mL) and dried in vacuo to afford $[Ru(CO)(PPh_3)_2(\eta^5\text{-}7,8\text{-}C_2B_9H_{11})]$ (**3a**) (436 mg, 88%). Calcd for $C_{39}H_{41}B_9OP_2Ru$: C, 59.4; H, 5.2. Found: C, 58.9; H, 4.9. IR: ν_{max}(CO) 1963 cm^{-1}, lit.[8] 1957 cm^{-1}.

(15) Evans, J.; Stroud, P. M.; Webster, M. *Organometallics* **1989**, *8*, 1270.
(16) Alexander, B. D.; Gomez-Sal, M. P.; Gannon, P. R.; Blaine, C. A.; Boyle, P. D.; Mueting, A. M.; Pignolet, L. H. *Inorg. Chem.* **1988**, *27*, 3301.
(17) Evans, D. G.; Mingos, D. M. P. *J. Organomet. Chem.* **1982**, *232*, 171.
(18) Hamilton, E. J. M.; Welch, A. J. *Polyhedron* **1990**, *9*, 2407.
(19) (a) Hallman, P. S.; Stephenson, T. A.; Wilkinson, G. *Inorg. Synth.* **1970**, *12*, 238. (b) McCleverty, J. A.; Wilkinson, G. *Inorg. Synth.* **1966**, *8*, 214.

Table 4. Selected Internuclear Distances (Å) and Angles (deg) for [RuCu(μ-H)(PPh$_3$)$_3$(η^5-7,8-C$_2$B$_9$H$_{11}$)]·2CH$_2$Cl$_2$·MeOH (**7a**)

Ru−C(1)	2.274(3)	Ru−C(2)	2.249(3)	Ru−B(4)	2.316(4)	Ru−B(3)	2.291(4)
Ru−B(5)	2.280(4)	Ru−P(2)	2.3042(10)	Ru−P(3)	2.3303(10)	Ru−H(001)	1.60(4)
Cu−H(4)	1.89(4)	Cu−P(1)	2.1838(10)	Ru−Cu	2.5758(6)	Cu−B(4)	2.215(4)
Cu−B(3)	2.445(4)	Cu−H(001)	1.89(4)	P(1)−C(11)	1.822(4)	P(1)−C(21)	1.828(4)
P(1)−C(31)	1.820(4)	P(2)−C(51)	1.845(4)	P(2)−C(41)	1.852(4)	P(2)−C(61)	1.860(4)
P(3)−C(71)	1.847(4)	P(3)−C(91)	1.852(4)	P(3)−C(81)	1.856(4)		

C(2)−Ru−C(1)	42.62(13)	C(2)−Ru−B(3)	44.47(14)	C(2)−Ru−B(5)	74.56(14)
C(1)−Ru−B(3)	74.90(14)	C(1)−Ru−B(5)	43.16(14)	B(5)−Ru−B(3)	78.2(2)
C(1)−Ru−P(2)	120.60(9)	C(2)−Ru−P(2)	163.18(10)	B(5)−Ru−P(2)	90.83(11)
B(3)−Ru−P(2)	141.45(11)	H(001)−Ru−P(2)	85.8(13)	H(001)−Ru−B(4)	99.5(13)
C(2)−Ru−B(4)	75.6(2)	C(1)−Ru−B(4)	74.81(14)	B(3)−Ru−B(4)	46.3(2)
B(5)−Ru−B(4)	46.2(2)	P(2)−Ru−B(4)	100.46(11)	H(001)−Ru−P(3)	80.1(13)
C(2)−Ru−P(3)	89.86(10)	C(1)−Ru−P(3)	98.49(9)	B(3)−Ru−P(3)	118.62(11)
B(5)−Ru−P(3)	135.64(11)	B(4)−Ru−P(3)	164.36(11)	P(2)−Ru−P(3)	95.11(3)
C(2)−Ru−Cu	104.30(9)	C(1)−Ru−Cu	126.32(9)	B(3)−Ru−Cu	59.99(11)
B(5)−Ru−Cu	97.11(11)	B(4)−Ru−Cu	53.53(11)	P(2)−Ru−Cu	85.45(3)
P(3)−Ru−Cu	127.15(3)	H(001)−Cu−P(1)	123.4(11)	H(001)−Cu−B(4)	94.3(11)
P(1)−Cu−B(4)	141.06(11)	P(1)−Cu−Ru	161.43(3)		

Table 5. Selected Internuclear Distances (Å) and Angles (deg) for [RuAu(μ-H)(PPh$_3$)$_3$(η^5-7,8-C$_2$B$_9$H$_{11}$)]·2CH$_2$Cl$_2$ (**8a**)

Ru−C(1)	2.249(6)	Ru−C(2)	2.237(6)	Ru−B(4)	2.323(7)	Ru−B(3)	2.260(7)
Ru−B(5)	2.322(7)	Ru−P(2)	2.334(2)	Ru−P(3)	2.363(2)	Ru−H(001)	1.79(6)
Au−H(001)	1.37(5)	Au−P(1)	2.252(2)	Au−Ru	2.7205(8)	P(1)−C(21)	1.808(7)
P(1)−C(31)	1.809(8)	P(1)−C(11)	1.821(7)	P(2)−C(61)	1.842(6)	P(2)−C(41)	1.846(6)
P(2)−C(51)	1.851(6)	P(3)−C(71)	1.856(6)	P(3)−C(81)	1.863(6)	P(3)−C(91)	1.827(6)

C(2)−Ru−C(1)	42.2(2)	C(2)−Ru−B(3)	45.2(2)	C(1)−Ru−B(3)	74.9(3)
C(2)−Ru−B(5)	74.8(2)	C(1)−Ru−B(5)	43.6(2)	B(3)−Ru−B(5)	78.0(3)
C(2)−Ru−B(4)	75.9(2)	C(1)−Ru−B(4)	75.0(2)	B(3)−Ru−B(4)	45.7(3)
H(001)−Ru−B(4)	77(2)	B(5)−Ru−B(4)	46.4(3)	H(001)−Ru−P(2)	87(2)
B(4)−Ru−P(2)	113.3(2)	C(2)−Ru−P(2)	96.8(2)	C(1)−Ru−P(2)	136.9(2)
B(3)−Ru−P(2)	82.5(2)	B(5)−Ru−P(2)	159.1(2)	H(001)−Ru−P(3)	99(2)
C(2)−Ru−P(3)	108.0(2)	C(1)−Ru−P(3)	87.6(2)	B(5)−Ru−P(3)	103.9(2)
B(4)−Ru−P(3)	149.1(2)	B(3)−Ru−P(3)	152.4(2)	P(2)−Ru−P(3)	96.89(6)
P(1)−Au−Ru	167.47(5)	H(001)−Au−P(1)	154(2)	P(2)−Ru−Au	113.44(4)
P(3)−Ru−Au	92.60(4)	C(1)−Ru−Au	109.1(2)	C(2)−Ru−Au	141.1(2)
B(4)−Ru−Au	70.1(2)	B(3)−Ru−Au	113.1(2)	B(5)−Ru−Au	68.3(2)

Synthesis of [RuRh(μ-H)(CO)(PPh$_3$)$_3$(η^5-7,8-C$_2$B$_9$H$_{11}$)]. A Schlenk tube containing **2b** (77 mg, 0.07 mmol) and [RhCl(CO)(PPh$_3$)$_2$] (50 mg, 0.07 mmol) was evacuated for 2 h to remove traces of oxygen. After addition of EtOH (10 mL) the mixture was stirred for 24−36 h, resulting in the gradual precipitation of a red solid from the colorless solution. Solvent was removed via a cannula and the crude solid redissolved in CH_2Cl_2 (ca. 5 mL), cooled to 0 °C, and left to stand overnight. The red-orange mixture thus obtained was passed through a short plug of silica (2 × 20 mm) using Et_2O as eluant. The filtrate thus obtained was layered with ethanol. On interdiffusion of the two solvents, deep red crystals of [RuRh(μ-H)(CO)(PPh$_3$)$_3$(η^5-7,8-C$_2$B$_9$H$_{11}$)] (**4**) formed, and these were washed with petroleum ether (1 × 10 mL) and dried under vacuum (44 mg, 81%). Calcd for $C_{57}H_{57}B_9OP_3RuRh\cdot 0.5CH_2Cl_2$: C, 57.7; H, 4.9. Found C, 57.8; H, 4.8. A side product (5−15%) was identified in the crude reaction mixture as **2d**, but since the latter decomposes during passage through silica, it is readily removed.

Synthesis of [Ru$_2$(μ-H)(H)(PPh$_3$)$_4$(η^5-7,8-C$_2$B$_9$H$_{11}$)]. Freshly prepared **2b** (244 mg, 0.23 mmol) was placed in a Schlenk tube with [RuCl$_2$(PPh$_3$)$_3$] (233 mg, 0.24 mmol) and the vessel evacuated to remove traces of air and moisture. Absolute ethanol (10 mL) was then added and the suspension gently warmed with stirring for ca. 5 h or until all [RuCl$_2$(PPh$_3$)$_3$] was consumed. After cooling, the mother liquor was removed and the remaining pale yellow solid was washed successively with H_2O (1 × 5 mL), chilled EtOH (1 × 10 mL) and Et_2O (1 × 10 mL) and dried under vacuum to afford [Ru$_2$(μ-H)(H)(PPh$_3$)$_4$(η^5-7,8-C$_2$B$_9$H$_{11}$)] (**5**) (250 mg, 78%). Samples thus prepared were sufficiently spectroscopically pure for subsequent syntheses.

Synthesis of [Ru$_2$(μ-H)(μ-σ:η^5-7,8-C$_2$B$_9$H$_{10}$)(CO)$_4$(PPh$_3$)$_2$]. Compound **5** (50 mg, 0.04 mmol) was placed in an Schlenk tube, which was evacuated. Dichloromethane (10 mL) previously saturated with CO was then added and the solution stirred under a brisk stream of CO gas for 12 h. The resultant pale yellow mixture was reduced in vacuo to ca. 2 mL and filtered through silica (20 × 50 mm) with Et_2O as eluant. Solvent was removed under vacuum and the residue dissolved in CH_2Cl_2 (ca. 2 mL). Slow diffusion into a pentane layer at 25 °C gave orange-red crystals, which were washed with petroleum ether and dried in vacuo to afford [Ru$_2$(μ-H)(μ-σ: η^5-7,8-C$_2$B$_9$H$_{10}$)(CO)$_4$(PPh$_3$)$_2$] (**6**) (33 mg, 94%). Calcd for $C_{42}H_{41}B_9O_4P_2Ru_2\cdot CH_2Cl_2$: C, 48.9; H, 4.1. Found: C, 49.2; H, 4.1.

Synthesis of the Complexes [RuM(μ-H)(L)(PPh$_3$)$_2$(η^5-7,8-C$_2$B$_9$H$_{11}$)] (M = Cu or Au, L = PPh$_3$ or CO). Compound **2b** (50 mg, 0.047 mmol) was placed in a Schlenk tube with [CuCl(PPh$_3$)$_3$] (42 mg, 0.047 mmol) and the vessel evacuated to remove all traces of oxygen. After addition of thf (10 mL) the solution was stirred for 12 h. Solvent was removed in vacuo and the residue redissolved in CH_2Cl_2 (ca. 2 mL) and layered with methanol. Diffusion of the two solvents gave bright yellow crystals, which were washed successively with methanol (2 × 10 mL) and petroleum ether (1 × 10 mL) and dried in vacuo to give [RuCu(μ-H)(PPh$_3$)$_3$(η^5-7,8-C$_2$B$_9$H$_{11}$)] (**7a**) (47 mg, 92%). Calcd for $C_{56}H_{57}CuB_9P_3Ru$: C, 61.0; H, 5.3. Found: C, 61.5; H, 5.4.

Similar procedures were followed for the synthesis of **7b**, **8a**, and **8b**. Thus by using **2d** (39 mg, 0.047 mmol) and [CuCl(PPh$_3$)$_3$] (0.047 mmol) pale yellow crystals of [RuCu(μ-H)(CO)(PPh$_3$)$_2$(η^5-7,8-C$_2$B$_9$H$_{11}$)] (**7b**) (39 mg, 97%) were obtained. Calcd for $C_{39}H_{42}CuB_9OP_2Ru\cdot CH_2Cl_2$: C, 51.0; H, 4.7. Found: C, 51.4; H, 4.7. IR (CH_2Cl_2): ν_{max}(CO) 1953 cm^{-1}. Similarly, reaction between **2b** (50 mg, 0.047 mmol) and [AuCl(PPh$_3$)] (23 mg, 0.047 mmol) gave yellow-orange crystals of [RuAu(μ-H)(PPh$_3$)$_3$(η^5-7,8-C$_2$B$_9$H$_{11}$)] (**8a**) (52 mg, 91%). Calcd for $C_{56}H_{57}AuB_9P_3Ru$: C, 55.2; H, 4.7. Found: C, 55.1; H, 4.8. Again substituting **2d** (39 mg, 0.047 mmol) afforded bright yellow crystals of [RuAu(μ-H)(CO)(PPh$_3$)$_2$(η^5-7,8-C$_2$B$_9$H$_{11}$)] (**8b**) (44 mg, 95%). Calcd for $C_{39}H_{42}AuB_9OP_2Ru\cdot CH_2Cl_2$: C, 44.9; H, 4.2. Found: C, 45.2; H, 4.3. IR (CH_2Cl_2): ν_{max}(CO) 1955 cm^{-1}.

Crystal Structure Determination and Refinements. Crystals of **3a** and **6** were grown from CH_2Cl_2−Et_2O, and those of **7a**, **7b**, and **8a** were grown from CH_2Cl_2−MeOH. The crystals were mounted on glass fibers. Low-temperature data were collected on a Siemens SMART

Table 6. Crystallographic Data for X-ray Crystal Structure Analyses

	3a	**6**·CH_2Cl_2	**7a**·$2CH_2Cl_2$·MeOH	**8a**·$2CH_2Cl_2$
formula	$C_{39}H_{41}B_9OP_2Ru$	$C_{43}H_{43}B_9Cl_2O_4P_2Ru_2$	$C_{59}H_{65}B_9Cl_4CuOP_3Ru$	$C_{58}H_{61}AuB_9Cl_4P_3Ru$
M_r	786.02	1056.04	1282.78	1388.10
T (°C)	−100	−100	−100	−100
space group	$P2_1/n$	$P2_1/c$	$P2_1/n$	$P2_1/c$
a (Å)	10.3868(10)	10.9437(14)	12.7415(10)	18.1297(38)
b (Å)	15.7892(16)	17.9009(41)	33.575(28)	18.0326(24)
c (Å)	22.8476(34)	23.8179(27)	14.0383(13)	18.3467(29)
β (deg)	91.633(13)	90.737(11)	96.628(8)	93.213(21)
V (Å^3)	3745.5(8)	4665.6(13)	5965.5(9)	5988.6(18)
Z	4	4	4	4
d_{calcd} (g cm^{-3})	1.394	1.503	1.428	1.540
μ(Mo Kα) (cm^{-1})	5.37	8.72	0.91	3.00
R1 (all data)[a]	0.0700	0.0466	0.0672	0.0806
wR2 (all data)[b]	0.0952	0.0668	0.0972	0.0992

[a] $R1 = \sum||F_o| - |F_c||/\sum|F_o|$. [b] $wR2 = [\sum\{w(F_o^2 - F_c^2)^2\}/\sum w(F_o^2)^2]^{1/2}$.

CCD area-detector three-circle diffractometer using Mo Kα X-radiation, $\lambda = 0.710\,73$ Å. For three settings of ϕ, narrow data "frames" were collected for 0.3° increments in ω. In all cases, a total of 1321 frames of data were collected, affording more than a hemisphere of data. It was confirmed that crystal decay had not taken place during the course of the data collections. The substantial redundancy in data allows empirical absorption corrections (SADABS)[20] to be applied using multiple measurements of equivalent reflections. The data frames were integrated using SAINT,[20] and the structures were solved by conventional direct methods. The structures were refined by full-matrix least-squares on all F^2 data using Siemens SHELXTL version 5.03,[20] with anisotropic thermal parameters for all non-hydrogen atoms. All calculations were performed on Dell PC, Silicon Graphics Indy, Indigo, or Iris computers.

For all structures, cage carbon atoms were assigned from the magnitudes of their anisotropic thermal parameters and from a comparison of the bond lengths to adjacent boron atoms. All hydrogen atoms, except for the Ru(μ-H)M hydrides in **6**, **7a**, and **8a**, and the agostic B−H⇀Cu hydrogen atom in **7a**, were included in calculated positions and allowed to ride on the parent boron or carbon atoms with fixed isotropic thermal parameters ($U_{iso} = 1.2U_{iso}$ of the parent atom except for methyl protons where $U_{iso} = 1.5U_{iso}$). The hydride H(3) of **6**, hydrides H(001) in **7a** and **8a**, and the agostic hydrogen H(4) in **7a** were located in difference Fourier syntheses and their positions and isotropic thermal parameter refined or fixed at $U_{iso} = 0.03$. For compound **7a** the chlorine atom of one CH_2Cl_2 molecule and the oxygen atom of the methanol molecule are disordered over two sites, 85:15 and 50:50, respectively. All the experimental data are summarized in Table 6.

Acknowledgment. We thank the Robert A. Welch foundation for support (Grant AA-1201).

Supporting Information Available: X-ray crystallographic data in CIF format for compounds **3a**, **6**·CH_2Cl_2, **7a**·$2CH_2Cl_2$·MeOH, **7b**·CH_2Cl_2, and **8a**·$2CH_2Cl_2$. This material is available free of charge via the Internet at http://pubs.acs.org.

IC990057Q

(20) *SHELXTL-PC*, version 5.03; Bruker AXS Inc.: Madison, WI, 1995.